Chapter 4

POD of 2D driven cavity

4.1 Introduction

In this chapter the POD eigenfunctions of the 2D driven cavity are discussed. These eigenfunctions are used to form the dynamical system of the next chapter. The data used to compute the POD have been supplied by a DNS (see Chapter 3). The Reynolds number at which the POD has been computed is Re=22,000. At this Reynolds number the flow in a 2D driven cavity is weakly turbulent.

An estimate for the (correlation) dimension of the strange attractor in this case has been determined in [60], the dimension was estimated at 10-20. This means that we have a low-dimensional chaotic flow.

In Section 4.2 the computed POD eigenvalues and eigenfunctions are discussed. In Section 4.2.1 a comparison with Fourier modes is made, to illustrate that POD modes are superior to Fourier modes as energy content is concerned. A reconstruction of an arbitrary fluctuating flowfield is made in Section 4.2.2.

4.2 POD eigenfunctions

The POD eigenfunctions have been computed for the DNS-database as presented in Chapter 3. The database consists of 700 snapshots each 5 time units apart, which is in the order of one large-eddy turn-over time. The computational method which we have used to compute the POD eigenfunctions is the so-called snapshot method. This method is described in Section 2.3. For the snapshot method we need uncorrelated snapshots. The correlation of subsequent snapshots in the DNS-database is less than 0.1 as shown in Fig. 4.1.

The number of 700 snapshots is chosen as large as reasonably possible for an accurate computation of the POD eigenfunctions. For the computation of only the first POD eigenfunctions we do not need to take 700 snapshots, because these first eigenfunctions, which correspond to high-energetic large-scale structures, can be formed with only a few snapshots. But for an accurate computation of low energy POD eigenfunctions a large number of snapshots is needed. We have computed the first 80 POD eigenfunctions. The convergence of the eigenvalues of the first 6 POD eigenfunctions is shown in Fig. 4.2

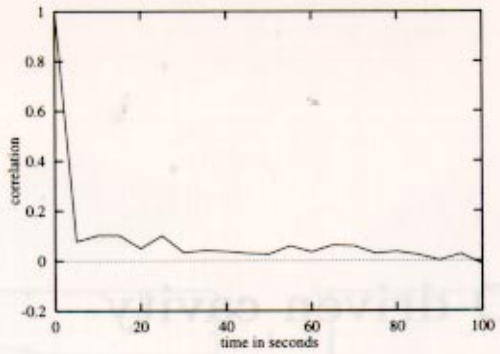

Figure 4.1: *Correlation of the 700 snapshots in the DNS-database.*

The eigenvalues are not fully converged. This is not too much of a problem since the POD eigenfunctions converge faster than the corresponding eigenvalues (see also Chapter 6). The properties of the POD eigenfunctions like orthogonality, divergence freeness, and satisfying the boundary conditions, are independent of the number of snapshots. When we use the POD eigenfunction for the dynamical system the eigenvalues are only important for the ordering of the POD eigenfunctions.

The eigenvalues are listed in Table 4.1. Note that the average amount of turbulent energy in the 'direction' of an eigenfunction is equal to the corresponding eigenvalue. The first eigenfunction contains 18% of the fluctuating kinetic energy. The first 20, 40 and 80 eigenfunctions contain (in time-average) 77%, 88% and 95% of the total fluctuating energy, respectively. The velocity fluctuations contain approximately 1.2 % of the total energy.

The first 12 eigenfunctions are shown in Fig. 4.3 and 4.4. It is well-known that Fourier modes can be grouped in pairs, e.g. $\sin(x)$ and $\cos(x)$ form a pair; they differ by a shift over one quarter of their period, and the rule $a\cos(x) + b\sin(x) = \sqrt{(a^2+b^2)}\cos(x \pm \delta)$ with $\tan(\delta) = \mp a/b$, provides the construction for a complete description of the evolution

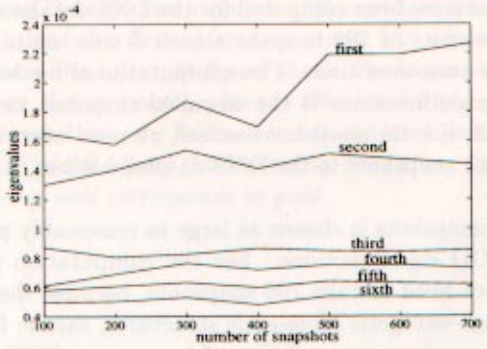

Figure 4.2: *Convergence of the eigenvalues as function of the number of snapshots*

index	λ_i	% energy
1	2.30765 10^{-4}	18.14
2	1.44456 10^{-4}	29.50
3	8.56222 10^{-5}	36.23
4	7.28991 10^{-5}	41.96
5	6.17286 10^{-5}	46.81
6	5.35092 10^{-5}	51.02
7	4.45789 10^{-5}	54.53
8	3.81593 10^{-5}	57.53
9	3.06833 10^{-5}	59.94
10	2.94565 10^{-5}	62.25
20	1.28227 10^{-5}	77.64
40	4.12892 10^{-6}	88.69
80	1.15345 10^{-6}	95.43

Table 4.1: *Some characteristic eigenvalues of the POD of the 2D driven cavity at Re=22,000. The right-hand column shows the relative energy of the projection of the fluctuating velocity field on the first i eigenfunctions (in time average).*

of a 'cosine-wave'. Fig. 4.3 suggests that POD-modes can be grouped in pairs, too. The first two form a pair. The second one is approximately a quarter out of phase compared to the first one. With the first two eigenfunctions only, a motion of an eddy in the lower-right corner of the cavity can be represented. Moreover, the third and fourth form a pair. With them an eddy moving in the lower part of the cavity can be represented.

The first two eigenfunctions clearly have the most energy in the lower-right corner. This means that the largest velocity fluctuations take place in that area of the cavity. The structures in the first eigenfunctions are large eddies indicating that large eddies have the most energy. The second pair of eigenfunctions has also a substantial amount of energy in the lower left corner. They are also large eddy-structures. The eddy-structures in the lower-right corner are smaller than those of the first pair of eigenfunctions.

The third pair of eigenfunctions looks like the second pair, but they are of course orthogonal to the second pair. The difference is that in the lower left corner the eddies turn in the same direction, but in the lower-right corner they are counter rotating.

The POD eigenfunctions with index 7 and 8 (see Fig. 4.4) do not clearly form a pair. The POD eigenfunctions with index 9 and 10 are the first eigenfunctions with high energy structures in the upper left corner of the cavity. They are also approximately a quarter out of phase. The fact that the first 8 eigenfunctions do not have high energy structures in this corner means that these structures do not possess much (fluctuating) energy. The structures in the upper left corner look like the structures in the lower-right corner of the first pair of eigenfunctions.

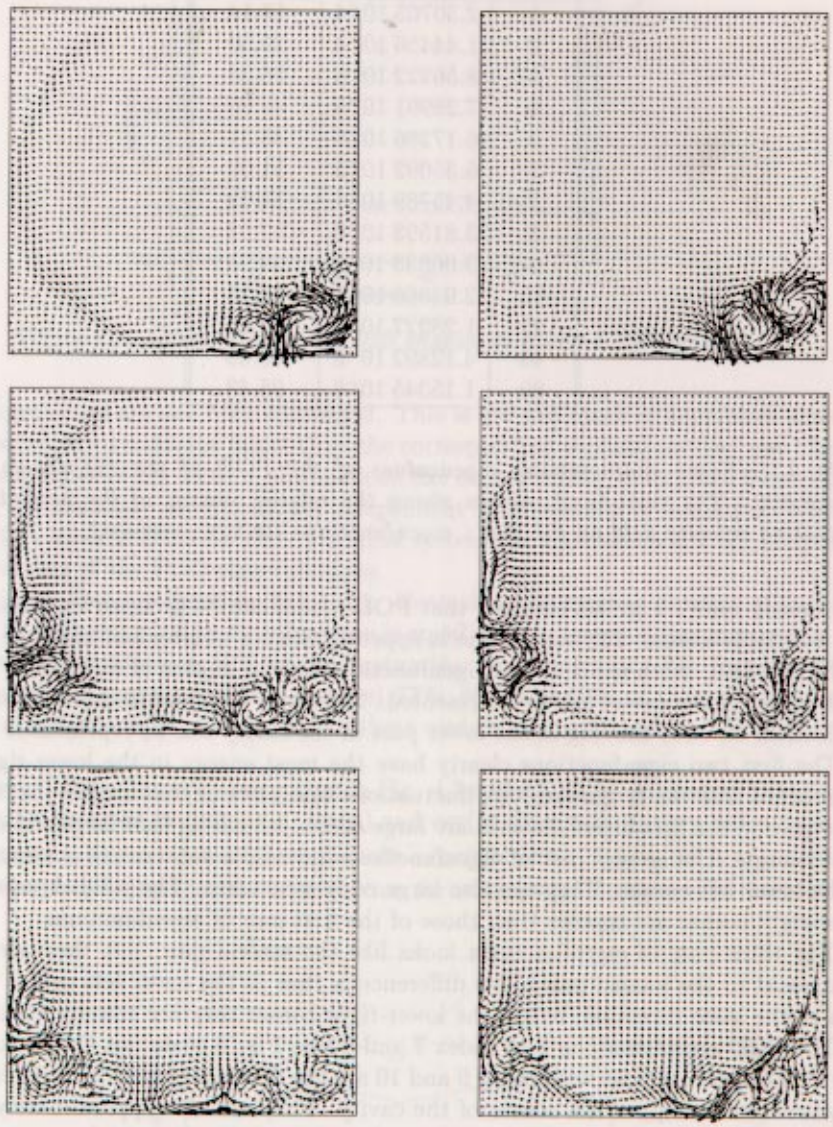

Figure 4.3: *Vector plots of the velocity of the first 6 POD eigenfunctions. The numbering goes in reading order.*

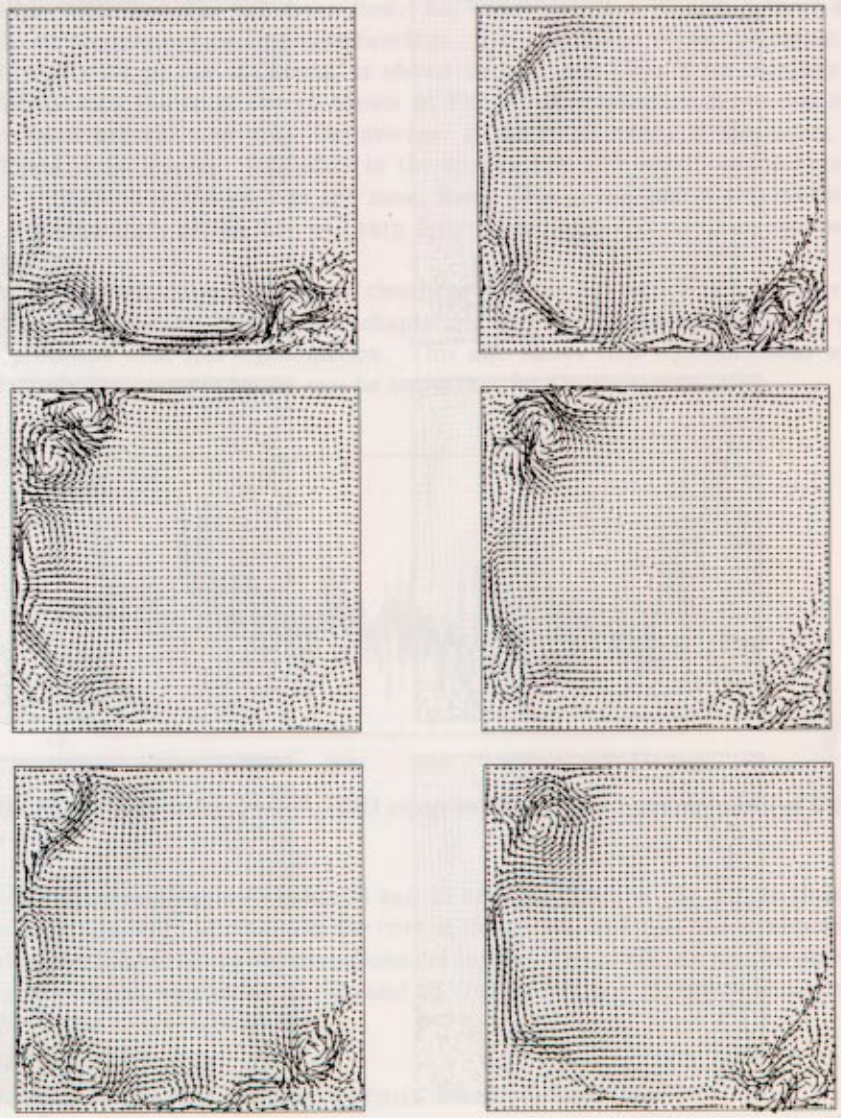

Figure 4.4: *Vector plots of the velocity of POD eigenfunctions 7 to 12. The numbering goes in reading order.*

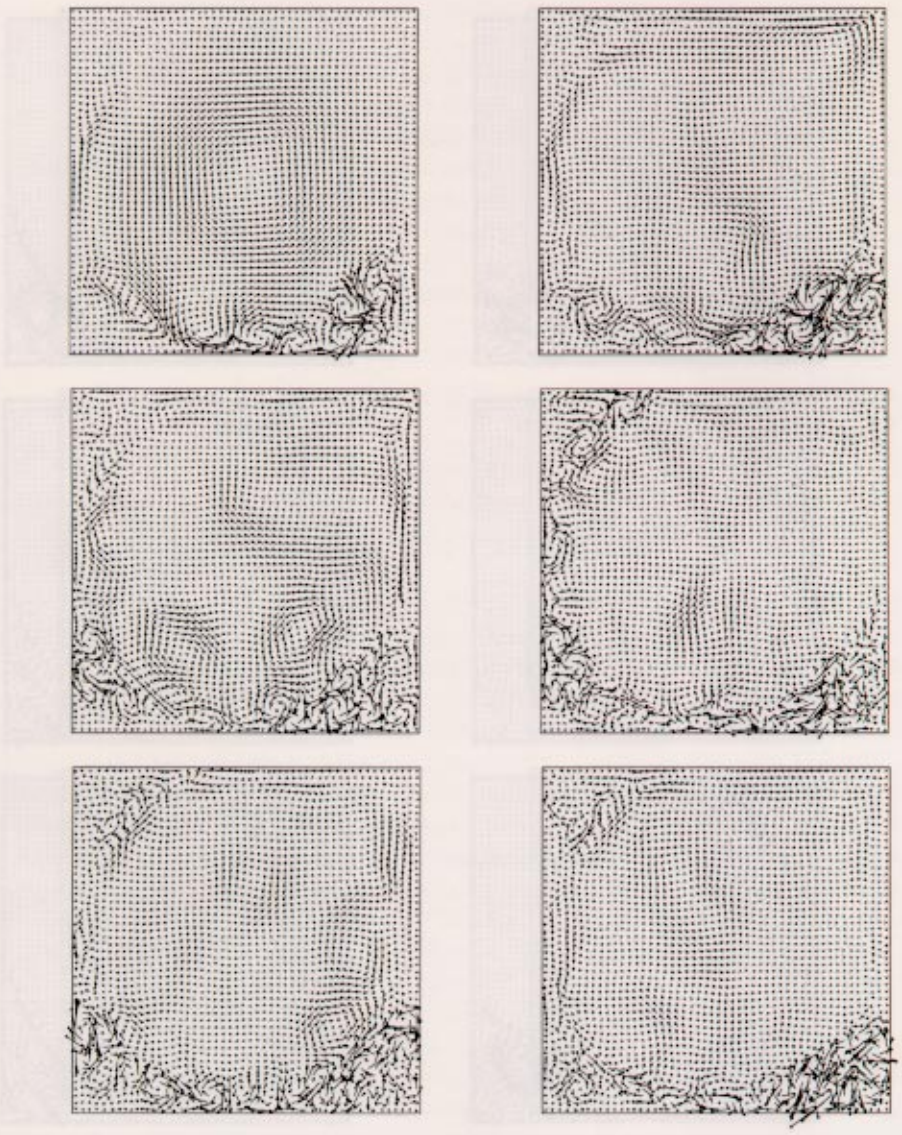

Figure 4.5: *Vector plots of the velocity of POD eigenfunctions 17,24,39,60,70, and 80. The numbering goes in reading order.*

The seventeenth POD eigenfunction, shown in Fig. 4.5, has a large eddy in the center of the cavity just like the mean flow. So, the fluctuation of such a large eddy will mainly be represented by this eigenfunction. The coefficient of this eigenfunction in the representation of the snapshots, is shown in Fig. 4.6. When we compare the 17^{th} coefficient with the total energy shown in Fig. 3.10 of Chapter 3, we can see a clear correlation between the two. On average, if the total energy is increasing, the 17^{th} coefficient is decreasing. The eddy in the core of the 17^{th} eigenfunction turns in the opposite direction of the eddy in the mean flow. This means that if this coefficient decreases the large eddy of the flow will turn faster. This corresponds to an increase of the total energy.

So, the 17^{th} eigenfunction corresponds clearly to a large time-scale which is important for the long-time dynamics. In the next chapter we will see that the dynamical system has some problems with this eigenfunction. This also shows that eigenfunctions which have a relatively low energy content can be important for the dynamics.

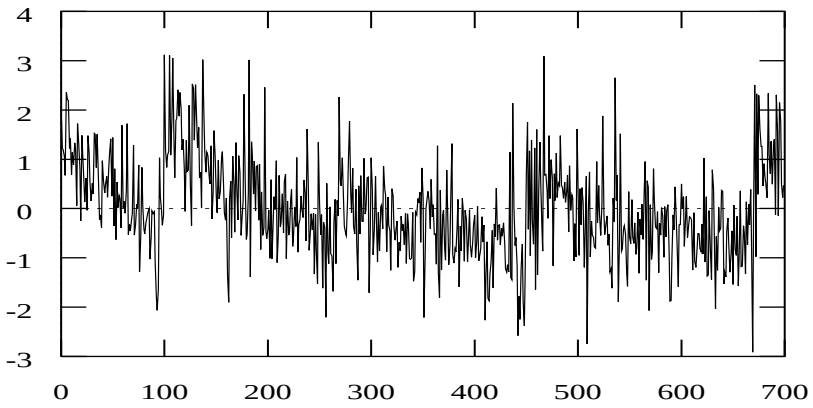

Figure 4.6: *The coefficient of the* 17^{th} *POD eigenfunction in the representation of the 700 snapshots*

The POD eigenfunctions with index 24 and 39 are also shown in Fig. 4.5, to illustrate that some have also large velocities in the core of the cavity, and that the structures get smaller when the indices of the eigenfunctions get higher. The latter can also be observed for the eigenfunctions with index 60, 70, and 80. In the last one almost no structure at all is visible in the lower-right corner.

4.2.1 POD eigenfunctions versus Fourier modes

POD eigenfunctions are optimal in the sense that every other set of the same number of modes contains less energy (in time average) than POD eigenfunctions do. To illustrate this we have compared the POD eigenfunctions with Fourier modes. The results are shown in Fig. 4.7. The Fourier modes are ordered according to increasing energy content. That means that we have first determined the energy content of the Fourier modes, and afterwards we have ordered them in increasing energy content. So, this is the most optimal ordering for the Fourier modes. As expected, the POD eigenfunctions converge much faster than the Fourier modes.

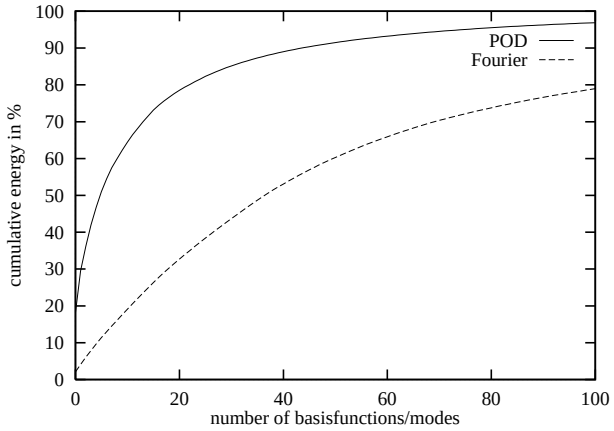

Figure 4.7: *Comparison of the energy content of the POD eigenfunctions and Fourier modes. The Fourier modes are ordered in increasing energy content. Clearly the energy content of the POD eigenfunctions is much larger.*

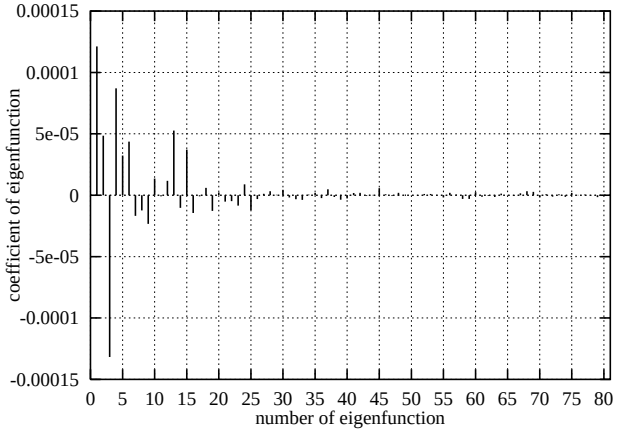

Figure 4.8: *Coefficients in the expansion of the arbitrary fluctuating velocity field of Fig. 4.9 in POD eigenfunctions.*

4.2.2 Reconstruction with POD eigenfunctions

The POD eigenfunctions converge optimally fast in L^2 norm in time average. But how fast does the reconstruction of an arbitrary velocity field converge? This depends of course on the velocity field. An example is shown in Fig. 4.9. In this figure only the fluctuations are shown, so the mean flow has been subtracted. The arbitrary fluctuating velocity field is shown in the lower-right picture, it comes from another simulation than the simulation which produced the snapshots for the POD. The first reconstruction is with the first 5 POD eigenfunctions. The most pronounced difference is the upper left corner of the cavity, where the projection on the first 5 POD eigenfunctions has small velocities and the full field has clearly an eddy-structure. This is no surprise, since the first 5 eigenfunctions do not have large velocities in the upper left corner (see Fig. 4.3).

Also the projection on the first 10 POD eigenfunctions does not show an eddy-structure in the upper-left corner, although large velocities are present in this corner in the eigenfunctions 9 and 10. In Fig. 4.8 is shown that the coefficients of the 9^{th} and 10^{th} POD

eigenfunctions are indeed relatively small. In this Fig. 4.8 we can also see that the third eigenfunction has a large contribution, in Fig. 4.3 we can see that the third eigenfunction 'looks' like the arbitrary fluctuating velocity field.

The projection on the first 20 eigenfunctions has an eddy-structure in the upper-left corner. All the large-scale structures are reasonably represented with only 20 POD eigenfunctions. When the number is increased from 20 to 40 to 80, the adjustments are small and concentrated on the small scales.

4.3 Conclusions

In this chapter we have presented the POD eigenfunctions for the 2D driven cavity. We have compared the energy content of the POD eigenfunctions with the energy content of Fourier modes. In Section 4.2.2 we have illustrated the convergence of the projection of an arbitrary velocity field on the POD eigenfunctions as a function of the number of eigenfunctions. The results lead to the following conclusions.

- From 500 to 700 snapshots the first 6 POD eigenvalues do not change much. So, we expect them to be more or less converged, even if we cover only twice a long time-scale with 700 snapshots.
- The first two POD eigenfunctions form a pair. With these two eigenfunctions a moving eddy in the lower-right corner can be represented. Also the third and fourth eigenfunctions form a pair.
- The seventeenth POD eigenfunction has a large eddy in the core of the cavity just like the mean flow. It appears that the process of building up energy and then dissipating it with an eddy in the core region corresponds to the long-term behavior of the coefficient of the seventeenth eigenfunction.
- The cumulative energy content of the first n POD eigenfunctions is much more than the cumulative energy content of the first n Fourier modes, even if the Fourier modes are ordered according to increasing energy content.

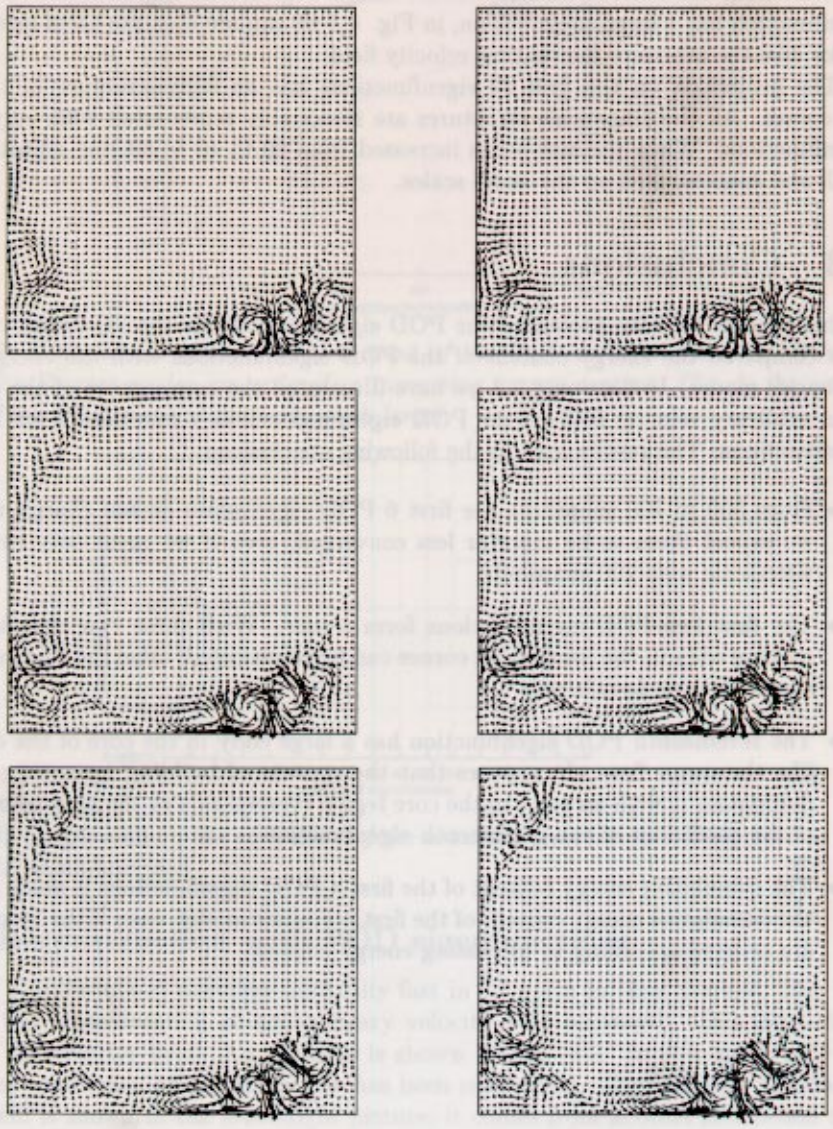

Figure 4.9: *Vector plots of projections on the first 5, 10, 20, 40, 80 POD eigenfunctions of an arbitrary velocity field. The mean flow has been subtracted. The arbitrary fluctuating velocity field is the lower-right picture, the others are projection on an in reading order increasing number of POD eigenfunctions.*